Low voltage reconfiguration: a comparison of metaheuristic and mathematical approaches

Sari Kerckhove*†‡, Reinhilde D'hulst†‡, Dirk Van Hertem*‡
*ESAT - Electa, KU Leuven, Leuven, Belgium
†VITO, Genk, Belgium
‡EnergyVille, Genk, Belgium

***Abstract*—The distribution system reconfiguration problem, which involves optimizing the topology of a power distribution network by determining switch-states, is a challenging combinatorial optimization problem with a large, nonconvex search space. For low voltage (LV) distribution networks, a solid comparison of various alternative optimization methods is lacking in literature. This paper aims to address this gap by comparing two different reconfiguration methods: a metaheuristic optimization approach based on a genetic algorithm formulation, and a mathematical optimization approach based on a second order cone relaxation of the exact formulation. Additionally, the significance of exploiting the low meshedness in LV-networks, by decoupling the network into independently reconfigurable subnetworks, is highlighted. The comparative analysis is done for a real European LV network which decouples into 164 subnetworks of varying combinatorial size. In addition to this, two medium voltage (MV) networks are also included in the comparison. The results robustly show the computational advantage of the genetic algorithm approach over the relaxed second order cone approach for networks with large combinatorial sizes, though the relaxed approach has the advantage of providing a lower bound to the global optimum.**

***Index Terms*—reconfiguration, low voltage distribution grids, method comparison, metaheuristic optimization, mathematical optimization**

I. Introduction

Power distribution networks typically have a meshed structure, though they generally are operated in radial configuration by opening and closing switches. Changing the state of these switches is known as distribution system reconfiguration (DSR). Reconfiguration is done to achieve multiple objectives such as reducing power losses, limiting network congestions, increasing hosting capacity, or enhancing voltage stability.

In European low voltage (LV) networks, considered in this paper, mainly manually controlled switches are present, hence network configurations are set for longer periods of time, referred to as static reconfiguration. However, despite its' potential to improve the usage of grid assets, numerous contacts with DSO's indicate that static reconfiguration is currently either little used or applied through suboptimal rules of thumb. Especially with the ongoing energy transition, resulting in an increased and more variable electricity demand and generation, it is increasingly important to optimally use existing infrastructure. Hence the development and application of optimal reconfiguration methods for LV distribution networks are indispensable.

A. Related literature

For medium voltage (MV) grids, reconfiguration is more common, and configuration optimization methods have been well-explored. DSR, with it's large scale, combinatorial nature, and nonlinear constraints, falls into the category of mixed-integer nonlinear programming (MINLP), and is therefore very challenging to solve. Since 1975, researchers have developed mathematical optimization, heuristic, and metaheuristic methods to tackle DSR [1].

Firstly, *mathematical programming approaches* usually obtain good quality solutions, often global optima, though generally at the cost of a high computation effort and time [1]. Exact formulations of the problem are nonlinear, hence they can not guarantee global optimality and often result in intractable computation times [2]. To alleviate this issue, the problem can be relaxed into convex problems such as the formulations proposed in [2] and [3]. The resulting solutions are often exact or at least can inform us on a lower bound to the objective. At the transmission level, the same relaxations have been successfully applied to the related transmission network expansion problem, also an MINLP, and similar conclusions were reached [4].

Secondly, *heuristic methods* are problem-specific and based on expert's experience and rules of thumb. They can be much faster than mathematical approaches, though they are greedy and can get stuck in local optima [1]. Early examples include the DISTOP and branch exchange method [5] [6], more recent heuristics to address DSR were proposed in [7] and [8].

Finally, *metaheuristic methods* are generic problem-solving frameworks inspired by physical or biological phenomena. Examples include genetic algorithms [9] [10], and particle swarm optimization [11]. Metaheuristic methods usually provide good-quality solutions through their explorative search, though no global optimality guarantee can be given. They have a higher computation cost than heuristics, but are often more tractable than mathematical approaches.

In summary, for MV networks, the general finding has been that mathematical programming methods, through relaxed formulations, can find optimal solutions to the DSR problem, or at least may provide a lower bound to the solution.

Submitted to the 23rd Power Systems Computation Conference (PSCC 2024).

However they can be time consuming especially for large networks. Metaheuristic methods on the other hand, require shorter computation time for large networks, while similarly obtaining good-quality results, though no global optimality guarantees can be given.

However, directly applying these conclusions for MV DSR on LV grids ignores the structural differences between LV and MV: LV networks generally contain many more feeders and are less meshed than MV networks, they have higher R/X-ratios, and their loads are more variable. Because of these differences, conclusions regarding the best DSR methods are not necessarily valid for LV grids.

B. Contributions and organization of the paper

The key contributions of the paper are:

- Providing a performance comparison between two DSR methods, a metaheuristic genetic algorithm (GA) approach with a mathematical second order cone (SOC) relaxation, to solve a real European LV test case. To the best of our knowlegde, such a comparison is missing for LV distribution nets.
- Exploiting typical LV network structure for reconfiguration: LV grids are less meshed and can be decoupled into independently reconfigurable subnetworks, significantly reducing the computational time of reconfiguration regardless of the chosen method.
- Categorization of the subnetworks by means of their combinatorial size, i.e. the number of possible radial configurations in the network, allows to meaningfully compare both approaches for different problem sizes.

The paper's structure is as follows: Section II details the reconfiguration problem; Section III presents both reconfiguration methods; Section IV explains how LV specific characteristics can be employed to improve DSR solution methods; Section V applies and compares the metaheuristic and mathematical method on a real LV network and two MV networks; and finally, Section VI concludes the study.

II. Distribution System Reconfiguration: Exact Problem Formulation

The reconfiguration problem considered in this paper aims to optimize the on/off states, α_{ij}, of all network switches to minimize network losses. Additionally, only radial network configurations are allowed, and voltage and current limits are imposed to prevent network congestion.

The exact formulation is described by Model 1. At the top, a description of input data and variables is given. $\mathcal{I}$ and $\mathcal{L}$ represent the set of buses and the set of directed lines in the network. $\mathcal{I}^{\text{ref}} \subset \mathcal{I}$ is the set of reference buses, which in this case corresponds to the buses located at each feeder-head. $\mathcal{L}^{\text{sw}} \subset \mathcal{L}$ represents the set of lines that include a switch. The objective (1.1) minimizes the total real power losses in the network. Constraints (1.2)-(1.4) ensure the power flow equations, expressed by a branch flow model (BFM) formulation. They consist of: power balance constraints (1.2), Ohm's law (1.3), and the power definition (1.4). Demand constraint (1.5)

Model 1: Exact DSR problem formulation (AC)

Inputs:

$\langle \mathcal{I}, \mathcal{I}^{\text{ref}}, \mathcal{L}, \mathcal{L}^{\text{sw}} \rangle$	- the power network
$z_{ij} \Leftrightarrow y_{ij}$	- impedance of line ij
s_i^d	- demands at bus i
$U_i^{\text{ref}}, U_i^{\max}, U_i^{\min}$	- voltage reference and limits at bus i
I_{ij}^{rated}	- current rating of line ij

Variables:

S_{ij}	- power flow on line ij
$\mathsf{s}_i = \mathsf{p}_i + j\mathsf{q}_i$	- power injection at bus i
U_i	- voltage at bus i
I_{ij}	- current through line ij
$\alpha_{ij} \in \{0,1\}$	- switch state of line ij
$\beta_{ij}, \beta_{ji} \in \{0,1\}$	- auxiliary variables at line ij

Minimal Loss Objective:

$$\min \sum_{i \in \mathcal{I}} \mathsf{p}_i \tag{1.1}$$

Power Flow Constraints:

$$\mathsf{s}_i = \sum_{j:ij\in\mathcal{L}} \alpha_{ij}\mathsf{S}_{ij} - \sum_{h:hi\in\mathcal{L}} \alpha_{hi}(\mathsf{S}_{hi} - z_{hi}|\mathsf{I}_{hi}|^2), \quad \forall i \in \mathcal{I}, \tag{1.2}$$

$$\mathsf{I}_{ij} = \alpha_{ij} y_{ij}(\mathsf{U}_i - \mathsf{U}_j), \qquad \forall ij \in \mathcal{L}, \tag{1.3}$$

$$\mathsf{S}_{ij} = \mathsf{U}_i \mathsf{I}_{ij}^*, \qquad \forall ij \in \mathcal{L}, \tag{1.4}$$

Demand Constraint:

$$\mathsf{s}_i = -s_i^d, \qquad \forall i \in \mathcal{I} \setminus \mathcal{I}^{\text{ref}}, \tag{1.5}$$

Voltage Constraints:

$$\mathsf{U}_i = U_i^{\text{ref}}, \qquad \forall i \in \mathcal{I}^{\text{ref}}, \tag{1.6}$$

$$U_i^{\min} \le |\mathsf{U}_i| \le U_i^{\max}, \qquad \forall i \in \mathcal{I} \setminus \mathcal{I}^{\text{ref}}, \tag{1.7}$$

Current Constraint:

$$|\mathsf{I}_{ij}| \le I_{ij}^{\text{rated}}, \qquad \forall ij \in \mathcal{L}, \tag{1.8}$$

Radiality Constraints:

$$\beta_{ij} + \beta_{ji} = \alpha_{ij}, \qquad \forall ij \in \mathcal{L}, \tag{1.9}$$

$$\sum_{j:ij\in\mathcal{L}} \beta_{ij} = 1, \qquad \forall i \in \mathcal{I} \setminus \mathcal{I}^{\text{ref}}, \tag{1.10}$$

$$\beta_{ij} = 0, \qquad \forall i \in \mathcal{I}^{\text{ref}}, \forall j : ij \in \mathcal{L}, \tag{1.11}$$

$$\alpha_{ij} = 1, \qquad \forall ij \in \mathcal{L} \setminus \mathcal{L}^{\text{sw}} \tag{1.12}$$

fixes the power injection to the given demand, such that only the power injection variables at the reference buses remain unknown. Constraint (1.6) sets the voltage at the reference buses to a preset reference value. Constraints (1.7) and (1.8) ensure reasonable voltage and current magnitude limits, these constraints are also referred to as the congestion constraints. Finally, radiality is enforced through radiality equations (1.9)-

(1.12). Switch state α_{ij} indicates the connectedness of line ij. Auxiliary variables β_{ij} and β_{ji}, indicate the parent-child relationship; if $i(j)$ is the parent of $j(i)$ then $\beta_{ij}(\beta_{ji}) = 1$. Equation (1.9) describes that there is only a parent-child relationship if the line is connected, and equations (1.10) and (1.11) indicate that each bus has exactly one parent, except the reference nodes which have none.

Some related notations are introduced as follows:

- A network configuration $\boldsymbol{\alpha} = [\alpha_{ij}]_{ij\in\mathcal{L}}$ with feasible, i.e. radial, configuration space $\mathcal{A}$

$$\mathcal{A} = \{\boldsymbol{\alpha} \mid \boldsymbol{\alpha} \text{ satisfying } (1.9) - (1.12)\} \tag{2}$$

- Network losses P_{loss}, i.e. the objective of the optimization problem (1.1) satisfying the power flow constraints:

$$P_{loss}(\boldsymbol{\alpha}) = \sum_{i\in\mathcal{I}} \mathsf{p}_i, \text{ satisfying } (1.2) - (1.6) \text{ for } \boldsymbol{\alpha} \tag{3}$$

We can directly provide Model 1 to an MINLP solver. While this exact AC approach is highly time-consuming and often fails to converge, when it does, it usually identifies the global optimum (though without guaranteed certainty). We denote the AC solution of the reconfiguration problem as $\boldsymbol{\alpha}_{\text{AC}}$. In this paper, $\boldsymbol{\alpha}_{\text{AC}}$ serves as the reference point for the solutions obtained through the metaheuristic and mathematical reconfiguration approaches introduced in the next section.

III. Optimal reconfiguration methods

A. Metaheuristic approach: Genetic Algorithm

This section presents a metaheuristic approach to solve the reconfiguration problem, more specifically a genetic algorithm. It is important to emphasize that, in the context of metaheuristics, the exact formulation presented in Model 1 is merely a description of the problem rather than being the input of any solver. Instead, the genetic algorithm (GA), described in Algorithm 1, iteratively searches the feasible, i.e. radial, configuration space $\mathcal{A}$. The search is guided towards optimality by a fitness function ϕ, introduced below, while simultaneously mutation and crossover operators introduce randomness to avoid ending up in local optima. The best configuration found by the GA method for a given DSR problem will be denoted by $\boldsymbol{\alpha}_{\text{GA}}$

In this case, the fitness of a configuration is defined as follows:

$$\phi(\boldsymbol{\alpha}) = -\left(\frac{P_{loss}(\boldsymbol{\alpha})}{P_{loss}(\boldsymbol{\alpha}_0)} + x^{\mathsf{U}} + x^{\mathsf{I}}\right). \tag{4}$$

$\phi(\boldsymbol{\alpha})$ is mostly determined by the active power losses $P_{loss}(\boldsymbol{\alpha})$, i.e. the objective of the optimization problem (1.1). Additionally, penalty terms for congestion constraint violations are added; x^{U} and x^{I} represent boolean values indicating respectively whether any of the voltage (1.7) or current congestion (1.8) constraints was violated. To achieve balance between the objective and the penalties, the power losses are normalized with the power losses of the default network configuration ($\boldsymbol{\alpha}_0$). The fitness sign is reversed such that lower losses correspond to higher fitness.

Algorithm 1: Genetic algorithm (GA)

Hyperparameters: p, g, P_e, P_m

- **Initialize** population of radial configurations through random spanning tree algorithm: $pop_0 \subset \mathcal{A}$, $|pop_0|= p$, $i = 0$.
- Determine fitness $\{\phi(\boldsymbol{\alpha}), \forall \boldsymbol{\alpha} \in pop_0\}$
- **While** $i <$ max no of generations g:
  - Selection: Favor $\boldsymbol{\alpha}$ with higher $\phi(\boldsymbol{\alpha})$ through elitism (elitism probability P_e) and binary tournament
  - Exploration: Apply radiality preserving mutation (mutation probability P_m) or crossover (remaining probability *1*-P_m) operators on selected configurations
  - $i = i + 1$, $pop_i = pop_{i-1}$
  - Determine fitness $\{\phi(\boldsymbol{\alpha}), \forall \boldsymbol{\alpha} \in pop_i\}$
- **End while**
- **Return** $\boldsymbol{\alpha} \in pop_i : \max \phi(\boldsymbol{\alpha})$

Note that, while not explicitly present in the fitness function, the power flow equations (1.2)-(1.6) are satisfied since they are calculated when P_{loss} is determined, as defined in (3). Moreover, the radiality constraints (1.9)-(1.12) are enforced since only radial configurations $\in \mathcal{A}$ are considered from the start. This is done by firstly using a random spanning tree initialization, and secondly by employing crossover and mutation operators that preserve radiality through maintaining the number of open switches (exchanging switch states in pairs) and assuring that no cycles are formed in this process of exchanging. This idea of radiality preserving operators was introduced in [12].

The hyperparameters of the GA method are the population size p, the number of generations g, the elitism probability P_e, and the mutation probability P_m.

B. Mathematical approach: Second Order Cone Relaxation

Alternatively to the metaheuristic approach (GA), a mathematical second order cone approach (SOC) is proposed in this section and written out in Model 2. The mixed-integer second order cone relaxation from [13] is applied to the exact problem in Model 1, expanding the feasible region such that it becomes convex, which allows to find a lower bound to the original problem. In practice, this lower bound and the exact solution are often found to coincide [2], [3].

To introduce the relaxed formulation, first a substitution of variables is required, replacing the complex voltage U_i and current I_{ij} with their respective squared magnitudes $\mathsf{u}_i = |\mathsf{U}_i|^2, \mathsf{l}_{ij} = |\mathsf{I}_{ij}|^2$. The voltage and current constraints (1.6)-(1.8) are replaced by their equivalent (5.4)-(5.6). The power flow equations, (1.2),(1.4) are replaced by (5.1)-(5.2) and the nonlinear constraint (6), which are equivalent for radial networks [13]:

$$|\mathsf{S}_{ij}|^2 = \mathsf{u}_i \mathsf{l}_{ij}, \forall ij \in \mathcal{L}. \tag{6}$$

Model 2: Second order cone relaxation (SOC)

Inputs: same as in Model 1

Variables: $\mathsf{S}_{ij}, \mathsf{s}_i, \alpha_{ij}, \beta_{ij}, \beta_{ji}$ from Model 1, and

u_i - squared voltage at bus i

l_{ij} - squared current through line ij

Minimal Loss Objective: (1.1) from Model 1

Power Flow Constraints:

$$\mathsf{s}_i = \sum_{j:ij\in\mathcal{L}} \alpha_{ij}\mathsf{S}_{ij} - \sum_{h:hi\in\mathcal{L}} \alpha_{hi}(\mathsf{S}_{hi} - z_{hi}\mathsf{l}_{hi}), \quad \forall i \in \mathcal{I}, \quad (5.1)$$

$$\alpha_{ij}(\mathsf{u}_i - \mathsf{u}_j) = 2\alpha_{ij}\Re(z_{ij}^*\mathsf{S}_{ij}) - |z_{ij}|^2\mathsf{l}_{ij}, \quad \forall ij \in \mathcal{L}, \quad (5.2)$$

$$|\mathsf{S}_{ij}|^2 \leq \mathsf{u}_i\mathsf{l}_{ij}, \quad \forall ij \in \mathcal{L}, \quad (5.3)$$

Demand Constraint: (1.5) from Model 1

Voltage Constraints:

$$\mathsf{u}_i = (U_i^{\text{ref}})^2, \quad \forall i \in \mathcal{I}^{\text{ref}}, \quad (5.4)$$

$$(U_i^{\text{min}})^2 \leq \mathsf{u}_i \leq (U_i^{\text{max}})^2, \quad \forall i \in \mathcal{I} \setminus \mathcal{I}^{\text{ref}}, \quad (5.5)$$

Current Constraint:

$$\mathsf{l}_{ij} \leq (I_{ij}^{\text{rated}})^2, \quad \forall ij \in \mathcal{L} \quad (5.6)$$

Radiality Constraints: (1.9)-(1.12) from Model 1

The second and last step in obtaining the SOC formulation in Model 2, is to make the feasible region convex by relaxing the nonlinear equality in (6) to an inequality resulting in second order cone constraint (5.3).

This relaxed mixed-integer second order cone problem can be solved with mixed-integer branch and bound approaches, binding the solution between an upper and lower bound up to a prescribed distance. The upper bound is the objective value of the best found radial solution $\boldsymbol{\alpha}_{\text{SOC}}$:

$$Obj_{\text{SOC}} = \sum_{i\in\mathcal{I}} \mathsf{p}_i, \text{ satisfying (5.1) – (5.6) for } \boldsymbol{\alpha}_{\text{SOC}}. \quad (7)$$

The lower bound LB_{SOC} is determined by the global optimum of the candidate node with the highest lower bound in the branch and bound. The maximum distance between upper and lower bound is set by the solver's hyperparameter MIPgap.

However, even if $LB_{\text{SOC}} = Obj_{\text{SOC}}$, the relaxation will still be inexact if the equality in (5.3) is not satisfied and therefore $Obj_{\text{SOC}} \neq P_{loss}(\boldsymbol{\alpha}_{\text{SOC}})$. In all cases, the losses of the optimal solution are guaranteed to be bounded by:

$$LB_{\text{SOC}} \leq P_{loss}(\boldsymbol{\alpha}_{\text{AC}}) \leq P_{loss}(\boldsymbol{\alpha}_{\text{SOC}}). \quad (8)$$

C. Performance indices

Numerical results use the following performance indices to assess the methods performance:

1) Computation time in seconds. t (s)
2) Absolute and relative loss reduction:

$$\Delta P_{loss}^{abs} = P_{loss}(\boldsymbol{\alpha}) - P_{loss}(\boldsymbol{\alpha}_0) \quad [kW], \quad (9)$$

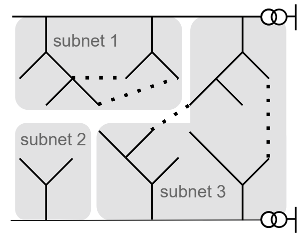

Fig. 1: Illustration of a network containing three subnetworks [14].

$$\Delta P_{loss}^{rel} = 100\left(1 - \frac{P_{loss}(\boldsymbol{\alpha})}{P_{loss}(\boldsymbol{\alpha}_0)}\right) \quad [\%]. \quad (10)$$

3) Optimality gap (%): the relative difference in losses with respect to the AC solution $\boldsymbol{\alpha}_{AC}$:

$$\text{Gap} = -100\left(1 - \frac{P_{loss}(\boldsymbol{\alpha})}{P_{loss}(\boldsymbol{\alpha}_{AC})}\right) \quad [\%]. \quad (11)$$

Alternatively, in absence of $\boldsymbol{\alpha}_{AC}$, the best found solution is used as a reference: $\min(P_{loss}(\boldsymbol{\alpha}_{GA}), P_{loss}(\boldsymbol{\alpha}_{SOC}))$.

4) Guaranteed maximal optimality gap (%). Only possible for SOC, based on the objective's lower bound LB_{SOC}:

$$\text{Gap}_{LB} = 100\left(1 - \frac{LB_{SOC}}{P_{loss}(\boldsymbol{\alpha}_{SOC})}\right) \quad [\%]. \quad (12)$$

IV. Low Voltage network characteristics

A. Subnetwork division

Before applying both methods introduced in section III, a closer look at the network properties is taken in this section, especially those properties that are specific to LV networks. In a large LV network, for example the network of a city, one single feeder can usually not be directly connected to all other feeders in the network by closing some switches. It is therefore often possible to subdivide the LV grid in subnetworks. Within one subnetwork, feeders can be directly connected by closing switches. However, no direct path, or switch, between the separate subnetworks exists. This idea is illustrated by Fig. 1. The subnetworks form independent reconfiguration problems as described in [14]. Decoupling the reconfiguration problem by independently reconfiguring the subnetworks can significantly improve the DSR's tractability or computation time.

The sizes of the subnetworks vary significantly for the testnetwork considered in this work. Generally, it can be assumed that in urban regions the networks are more meshed, and larger subnetworks will exist, while in rural regions less or no reconfiguration options exist, corresponding to small or single-feeder subnetworks. In contrast to LV networks, MV networks are often more meshed and do not usually decouple into many independent subproblems.

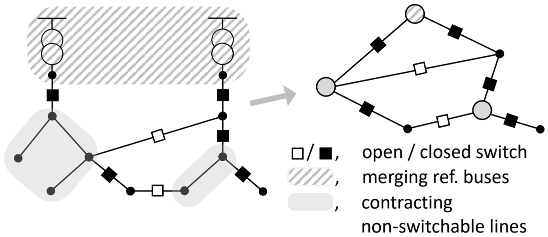

Fig. 2: Reducing the network graph for counting the number of radial configurations through Kirchhoff's matrix tree theorem.

TABLE I: Properties of the test networks: nominal voltage, number of feeders, switches, radial options, and subnets.

	U^{nom} (kV)	$\lvert\mathcal{I}^{\text{ref}}\rvert$	$\lvert\mathcal{L}^{\text{sw}}\rvert$	$\lvert\mathcal{A}\rvert$	|subnets|
LV 3800-bus net	0.23	252	534	$3\ 10^{62}$	164
MV 84-bus net	11.4	11	89	$4\ 10^{11}$	2
MV 136-bus net	13.8	8	118	$2\ 10^{18}$	1

B. Combinatorial size

Because network size can significantly impact different reconfiguration methods performance, it is necessary to take network size into account when comparing methods. For this paper, we propose to categorize the networks by their number of possible radial options $|\mathcal{A}|$, which will be called the combinatorial size. In contrast to categorizing in terms of number of feeders or number of switches, the combinatorial size gives a clearer picture of the problem's actual complexity.

The combinatorial size can be calculated by means of Kirchhoff's matrix tree theorem from graph theory. In graph theory, the concept of radiality is equivalent to the concept of spanning trees. Kirchhoff's matrix tree theorem shows that the number of spanning trees in a graph can be computed from the Laplacian matrix of this graph, specifically the number of trees equals any cofactor of this Laplacian matrix [15] [16].

Kirchhoff's theorem can not be directly applied to the original network graph because it is designed for spanning trees with a single root, while a radial configuration typically corresponds to a spanning forest with multiple roots (the reference buses). Additionally, Kirchhoff's theorem does not consider the constraint that all non-switchable lines must always be present in any radial solution. To address these issues, a reduced graph is created, as illustrated in Fig. 2, by firstly merging all reference buses into one root-node, and secondly by contracting all non-switchable lines into a single node. This reduced graph retains the same number of possible radial configurations $|\mathcal{A}|$ as the original network graph while allowing direct application of Kirchoff's theorem.

In what follows, combinatorial size $|\mathcal{A}|$ will be used to categorize the networks.

V. Numerical Test Case

A. Description of Test Setup

a) Network data: The proposed metaheuristic and mathematical reconfiguration methods are compared for three test networks consisting of one LV network, a 3800-bus (0.23 kV)

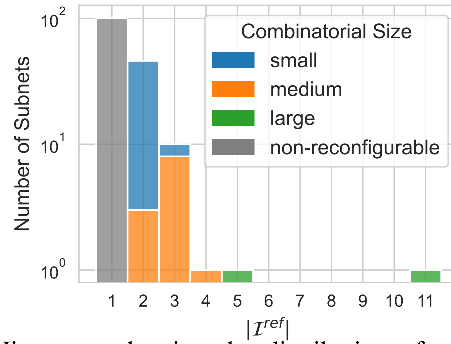

Fig. 3: Histogram showing the distribution of subnetworks with respect to their number of feeders $|\mathcal{I}^{\text{ref}}|$ [14].

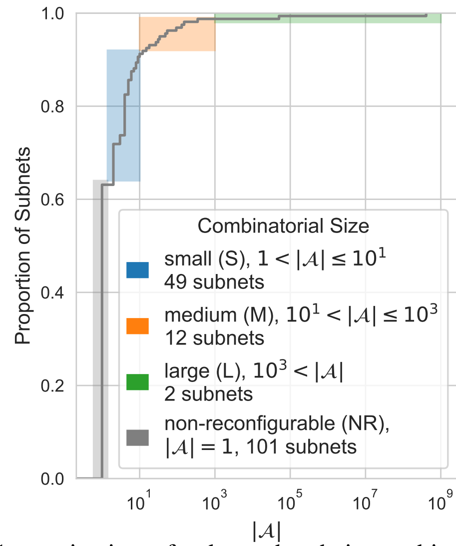

Fig. 4: Categorization of subnets by their combinatorial size $|\mathcal{A}|$, illustrated on the empirical cumulative distribution.

Spanish network described in [17], and two MV networks, the 83-bus (11.4 kV) and 136-bus (13.8 kV) networks introduced in [18] and [19]. Their main properties are listed in Table I.

The demand inputs s_i^d of the LV grid correspond to the average of a 20 day load measurement series from [17]. For the MV grids, the demand inputs correspond to the demands given in [18] and [19]. The voltages are expressed per unit with $U_i^{\text{ref}} = 1$, and limits $U_i^{\min} = 0.9, U_i^{\max} = 1.1$. The rated current I_{ij}^{rated} is a line dependent parameter.

TABLE II: Two versions of the GA reconfiguration method with different hyperparameters: (p, g)

		GA1 (p, g)	GA2 (p, g)
LV subnets	$\lvert\mathcal{I}^{\text{ref}}\rvert$=1	-	-
	$\lvert\mathcal{I}^{\text{ref}}\rvert$=2	(7, 15)	(7, 8)
	$\lvert\mathcal{I}^{\text{ref}}\rvert$=3	(10, 30)	(10, 15)
	$\lvert\mathcal{I}^{\text{ref}}\rvert$ >3	(15, 60)	(15, 30)
LV net		(20, 175)	(20, 125)
MV 84-bus net		(15, 110)	(15, 80)
MV 136-bus net		(20,200)	(20, 150)

b) LV Subnetworks and categorization: The LV network consists of 164 subnetworks, with the subnetworks defined as in Section IV-A. In Fig. 3, a histogram shows the subnetworks' distribution with respect to their number of reference buses. Remarkably, from the 164 subnetworks, there are 101 single-feeder subnetworks which can not be further reconfigured, hence only 63 reconfigurable subnetworks remain, and only 3 of them contain more than 3 feeders. As indicated in Section IV-B, these reconfigurable subnetworks are categorized by their combinatorial size $|\mathcal{A}|$. This categorization is illustrated in Fig. 4. Apart from the non-reconfigurable subnets ($|\mathcal{A}|$=1), three size categories are defined: small ($|\mathcal{A}| \leq$10), medium (10$<|\mathcal{A}| \leq 10^3$), and large ($|\mathcal{A}| > 10^3$), containing respectively 49, 12, and 2 subnets.

In contrast, as can be seen in Table I, the 83- and 136-bus MV networks only have 2 and 1 subnetworks due to their meshedness. Consequently, they also have larger combinatorial sizes, $4{\cdot}10^{11}$ and $2{\cdot}10^{18}$ respectively. Additionally, the non-decoupled LV network is also listed in Table I. Notice that it's combinatorial size ($3{\cdot}10^{62}$) is many orders of magnitude larger than the size of it's largest subnet ($4{\cdot}10^8$). This highlights the critical role of decoupling in reducing computational demands.

c) Implementation: All calculations described in this work are performed on a 64-bit machine with Intel(R) Core(TM) i5-10310U CPU @ 1.70GHz and 8 GB RAM. The AC and SOC methods are implemented in the PowerModels.jl framework [20], using the Julia programming language. The AC method uses the Juniper solver, which relies on Gurobi as mixed-integer solver and Ipopt as nonlinear solver. Meanwhile, the SOC method employs Gurobi as its solver. The GA framework is implemented in Python and uses a self-implemented backward forward sweep method to calculate the power flows in each iteration.

The values of the hyperparameters for the genetic algorithm: population size p, maximum number of generations g, mutation probability P_m, and elitism probability P_e are chosen empirically. P_m and P_e are set at 70% and 30% respectively, while p and g are network dependent, and their values are listed in Table II. Two hyperparameter scenarios are tested, resulting in two variations of the metaheuristic reconfiguration method. The first one, GA1, has a larger maximum generation number and therefore gets a longer time to converge, it is therefore more conservative than the second method, GA2. Notice that non-reconfigurable, single-feeder subnetworks do not need hyperparameters. For the SOC method, the gap tolerance, MIPgap, is set at 0.01%.

d) Case studies: Two case studies will be described:

- Case study 1: Comparison of the GA1, GA2, and SOC methods' performanc on the LV subnetworks of varying combinatorial sizes.
- Case study 2: Comparison of the GA1, GA2, and SOC methods' performance for both LV and MV networks.

B. Case study 1: Method comparison for LV subnetworks

a) Loss reduction and optimality gap: Fig. 5a shows the distribution of the default losses for each of the subnets $P_{loss}(\boldsymbol{\alpha}_0)$, which sum up to a total loss of 30.70 kW as reported in Table III. For the reconfigurable subnets, Fig. 5b shows the absolute loss reduction $\Delta P^{abs}_{loss}(\boldsymbol{\alpha})$ for each subnet and each method, summing up to 9.03 kW for GA1, 9.00 kW for GA2, and 9.03 kW for SOC for the total LV network. Though GA2 scores a tiny bit less, the results look almost indistinguishable. It can be concluded that all methods have practically the same performance in terms of minimizing losses.

In Fig. 5d the optimality gap, Gap, is shown, illustrating how GA1 and SOC reach global optimality (Gap=0) for all subnets, while GA2 is globally optimal for the small and medium subnets, and within (Gap$<$0.5%) for the large subnets. On a side note, it is worth mentioning that in several cases, multiple solutions were identified as globally optimal, with accuracy up to 10^{-6} kW. This suggests a flat optimal surface for the LV subnets.

The maximal gap guaranteed for SOC, Gap_{LB} is given in Fig. 5e. Because LB_{SOC} is a lower bound, Gap_{LB} should always be positive. However, slight negative values are found as well, which might be due to the inequality tolerance within the solver. For the total LV network, it can be concluded that SOC guarantees global optimality within an uncertainty range of 0.01%.

b) Computation time: In Fig. 5c the computation time per subnet, per method is given. A first observation is that the computation time is clearly correlated to the subnet's combinatorial size category, notice that the time-axis is logarithmic. Allowing to meaningfully compare results per category.

- Large subnets ($|\mathcal{A}| > 10^3$): GA1 and GA2 are significantly faster than SOC.
- Medium subnets (10$<|\mathcal{A}| \leq 10^3$): GA2 is comparable (usually slightly faster, sometimes slightly slower) to SOC computation, GA1 is slightly slower.
- Small subnets ($|\mathcal{A}| \leq$10): SOC is mostly faster than GA1 and GA2, however in these cases, a simple enumeration of the feasible configurations might be a more efficient way to determine the best configuration.

In addition to the GA1, GA2 and SOC results, Fig. 5c also shows the much longer computation times for the AC method. The three largest subnets did not converge for the AC method as the iteration limit was reached. As listed in Table III, the overall computation times sum up to 65 s for GA1, 31 s for GA2, and 347 s for SOC. The halving of computation time from GA1 to GA2 illustrates the importance of hyperparameter-tuning. Finally, Table III shows the infeasibliity of the non-decoupled approach, as it takes 12 times longer than the decoupled scenario for GA and exceeds the time limit for SOC.

c) Discussion: Since the large subnets contribute most to the computation time, GA2 provides a factor 10 speedup with respect to SOC, and is therefore recommended. However, if computation time is less important and a guarantee on the maximal gap is preferred, SOC should be used.

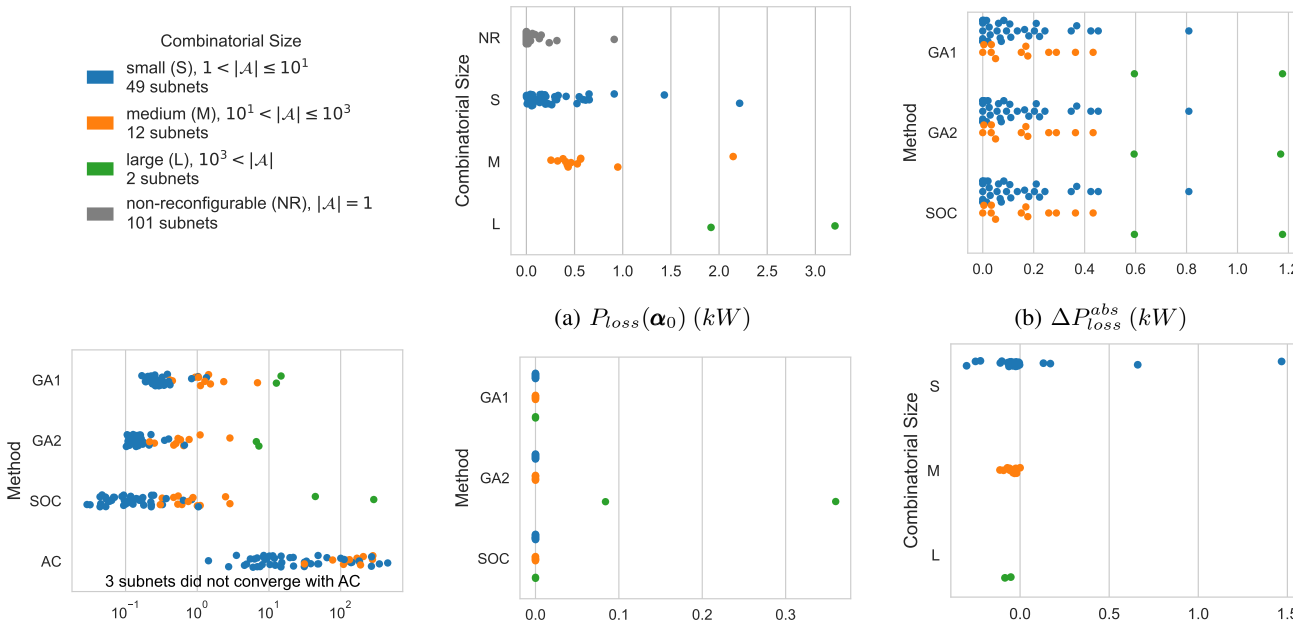

(a) $P_{loss}(\boldsymbol{\alpha}_0)$ (kW) (b) ΔP_{loss}^{abs} (kW)

(c) t (s) (d) Gap (%) (e) Gap$_{LB}$ (%)

Fig. 5: Performance of all methods for each of the subnetworks, categorized by combinatorial size.

Because these results were based on a LV network with 164 diverse subnets, this conclusion is expected to be robust and the methods are likely to behave similar on new LV subnets.

C. *Case study 2: Method comparison for LV and MV networks*

a) Loss reduction and optimality gap: Table III shows that for both the 84-bus network and the 136-bus network all three methods have similar performance in terms of loss reduction, respectively 11.9 % and 12.5 % with optimality gaps lower than 0.02 % and 0.1 % respectively. The AC solution was only found for the 84-bus network, while the time limit was exceeded for 136-bus network. The maximal gap Gap$_{LB}$ guaranteed by SOC is higher for these MV networks than they were for the LV subnets, though they are still very small: 1.17 % and 0.64 % respectively.

b) Computation time: Computation times are again evaluated in relation to the networks' combinatorial sizes:

- 136-bus net ($|\mathcal{A}| = 2{\cdot}10^{18}$): GA2 (GA1) is 2.5 (2) times faster than SOC.
- 84-bus net ($|\mathcal{A}| = 4{\cdot}10^{11}$): The SOC method is 3 (4) times faster than GA2 (GA1).

c) Discussion: So both for the LV subnetworks and the MV networks the trend seems to be that SOC method is faster for networks with smaller combinatorial size, while the metaheuristic method GA2 is faster for networks with larger combinatorial size. However, the size at which the GA2 overtakes SOC in computation time differs greatly for the LV and MV networks. The SOC method was still 3 times faster than GA2 for the 84-bus network, while it's size, $|\mathcal{A}| = 4{\cdot}10^{11}$, is larger than any of the LV subnets.

TABLE III: Computation time, loss reduction, and (guaranteed) optimality gap for each network, and for all methods.

		t (s)	P_{loss} (kW)	$\Delta P_{\text{loss}}^{\text{rel}}$ (%)	Gap (%)	Gap$_{LB}$ (%)
LV net decoupled $|\mathcal{A}| \leq 4 \cdot 10^8$	$\boldsymbol{\alpha}_0$	-	30.70	-	-	-
	GA1	65	21.68	29.4	0	-
	GA2	31	21.69	29.3	0.05	-
	SOC	347	21.68	29.4	0	0±.01
	AC	*it. limit*	not all (60/63) subnets converged			
not decoupled $|\mathcal{A}| = 3 \cdot 10^{62}$	GA1	748	21.95	28.5	1.25	-
	GA2	503	22.28	27.4	2.77	-
	SOC	>3600	*n.a.*	*n.a.*	*n.a.*	*n.a.*
	AC	>3600	*n.a.*	*n.a.*	*n.a.*	-
MV net 84-bus $|\mathcal{A}| = 4 \cdot 10^{11}$	$\boldsymbol{\alpha}_0$	-	531.99	-		-
	GA1	12	469.88	11.68	0	-
	GA2	10	469.97	11.66	0.02	-
	SOC	3	469.88	11.68	0	1.17
	AC	1225	469.88	11.68	0	-
MV net 136-bus $|\mathcal{A}| = 2 \cdot 10^{18}$	$\boldsymbol{\alpha}_0$	-	320.3	-	-	-
	GA1	47	280.1	12.5	0	-
	GA2	40	280.6	12.4	0.1	-
	SOC	105	280.2	12.5	0	0.64
	AC	>3600	*n.a.*	*n.a.*	*n.a.*	-

The reason for this difference between LV and MV is not entirely clear. The findings in Section V-B, which reveal flat optimal surfaces in LV networks, might offer an explanation as to why MV networks appear to be more amenable to mathematical approaches compared to LV networks.

VI. Conclusion

This paper provides a performance comparison between two distribution grid reconfiguration methods, one metaheuristic genetic algorithm (GA) approach, and one mathematical second order cone (SOC) relaxation, on a real European LV test case.

Because LV networks are inherently less meshed than MV networks, decoupling of LV networks into independently reconfigurable subnetworks can be exploited. Regardless of the reconfiguration method, this decoupling allowed significant computational speedup for LV reconfiguration: The GA method achieved a 12-fold speedup, and issues with exceeding time limits for the SOC method were resolved.

To meaningfully compare both methods for different network sizes, the 164 LV subnets resulting from the decoupling were categorized by means of their combinatorial size. For all size categories, both methods perform very well in terms of loss minimization, with an optimality gap consistently below 0.5%. However, computation times vary: SOC is faster for small combinatorial sizes (<10), GA is comparable or slightly faster for medium sizes (10-1000), and GA significantly outperforms SOC for large sizes (>1000). Notably, careful hyperparameter tuning is needed for optimal GA performance. Because these results were derived from 164 diverse subnets, this conclusion is robust. As the large subnets contribute most to the computation time, GA achieves an overall computation time that is 10-fold faster than SOC.

For the MV networks, though only two networks were considered, the trend again seems to be that GA method is faster for larger networks than the SOC method. However, surprisingly, the size at which GA overtakes SOC in speed is many orders of magnitude larger than for LV networks.

We conclude that, specifically for the reconfiguration of LV networks, decoupling into subnetworks is indispensable. Additionally, the metaheuristic GA method is recommended over the mathematical SOC method providing a signigicant computational speedup. However, if computation time is of lesser concern, SOC provides the advantage of guaranteeing a tight lower bound (<1%) to the found solution.

Acknowledgments

This research was funded by an FWO-Flanders grant (1SA7222N) for strategic basic research.

References

[1] M. Mahdavi, H. H. Alhelou, N. D. Hatziargyriou, and F. Jurado, "Reconfiguration of electric power distribution systems: Comprehensive review and classification," *IEEE Access*, vol. 9, pp. 118 502–118 527, 2021.

[2] C. L. Silveira, A. Tabares, L. T. Faria, and J. F. Franco, "Mathematical optimization versus Metaheuristic techniques: A performance comparison for reconfiguration of distribution systems," *Electric Power Systems Research*, vol. 196, no. October 2020, 2021.

[3] R. A. Jabr, R. Singh, and B. C. Pal, "Minimum loss network reconfiguration using mixed-integer convex programming," *IEEE Transactions on Power Systems*, vol. 27, no. 2, pp. 1106–1115, 2012.

[4] R. Bent, C. Coffrin, R. R. E. Gumucio, and P. Van Hentenryck, "Transmission network expansion planning: Bridging the gap between ac heuristics and dc approximations," in *2014 Power Systems Computation Conference*, 2014, pp. 1–8.

[5] D. Shirmohammadi and H. Hong, "Reconfiguration of electric distribution networks for resistive line losses reduction," *IEEE Transactions on Power Delivery*, vol. 4, no. 2, pp. 1492–1498, 1989.

[6] M. Baran and F. Wu, "Network reconfiguration in distribution systems for loss reduction and load balancing," *IEEE Transactions on Power Delivery*, vol. 4, no. 2, pp. 1401–1407, 1989.

[7] N. V. Kovački, P. M. Vidović, and A. T. Sarić, "Scalable algorithm for the dynamic reconfiguration of the distribution network using the lagrange relaxation approach," *International Journal of Electrical Power & Energy Systems*, vol. 94, pp. 188–202, 2018. [Online]. Available: https://www.sciencedirect.com/science/article/pii/S0142061516321019

[8] X. Ji, Q. Liu, Y. Yu, S. Fan, and N. Wu, "Distribution network reconfiguration based on vector shift operation," *IET Generation, Transmission and Distribution*, vol. 12, no. 13, pp. 3339–3345, 2018.

[9] K. Nara, A. Shiose, M. Kitagawa, and T. Ishihara, "Implementation of genetic algorithm for distribution systems loss minimum reconfiguration," *IEEE Transactions on Power Systems*, vol. 7, no. 3, pp. 1044–1051, 1992.

[10] A. M. Eldurssi and R. M. O'Connell, "A fast nondominated sorting guided genetic algorithm for multi-objective power distribution system reconfiguration problem," *IEEE Transactions on Power Systems*, vol. 30, no. 2, pp. 593–601, 2015.

[11] H. Wu, P. Dong, and M. Liu, "Distribution network reconfiguration for loss reduction and voltage stability with random fuzzy uncertainties of renewable energy generation and load," *IEEE Transactions on Industrial Informatics*, vol. 16, no. 9, pp. 5655–5666, 2020.

[12] B. Enacheanu, B. Raison, R. Caire, O. Devaux, W. Bienia, and N. HadjSaid, "Radial network reconfiguration using genetic algorithm based on the matroid theory," *IEEE Transactions on Power Systems*, vol. 23, no. 1, pp. 186–195, 2008.

[13] S. H. Low, "Convex relaxation of optimal power flow—part i: Formulations and equivalence," *IEEE Transactions on Control of Network Systems*, vol. 1, no. 1, pp. 15–27, 2014.

[14] S. Kerckhove, R. D'Hulst, and D. Van Hertem, "Reconfiguration method for low voltage distribution networks," 2023, submitted to *2023 IEEE PES Innovative Smart Grid Technologies Europe (ISGT-Europe)*.

[15] H. M. Trent, "A note on the enumeration and listing of all possible trees in a connected linear graph," *Proceedings of the National Academy of Sciences*, vol. 40, no. 10, pp. 1004–1007, 1954. [Online]. Available: https://www.pnas.org/doi/abs/10.1073/pnas.40.10.1004

[16] "Kirchhoff's theorem," Apr. 2023. [Online]. Available: https://en.wikipedia.org/w/index.php?title=Kirchhoff%27s_theorem&oldid=1148304238

[17] A. Koirala, L. Suárez-Ramón, B. Mohamed, and P. Arboleya, "Non-synthetic european low voltage test system," *International Journal of Electrical Power & Energy Systems*, vol. 118, p. 105712, 2020. [Online]. Available: https://www.sciencedirect.com/science/article/pii/S0142061519318836

[18] C.-T. Su and C.-S. Lee, "Network reconfiguration of distribution systems using improved mixed-integer hybrid differential evolution," *IEEE Transactions on Power Delivery*, vol. 18, no. 3, pp. 1022–1027, 2003.

[19] J. R. Mantovani, F. Casari, and R. A. Romero, "Reconfiguração de sistemas de distribuição radiais utilizando o critério de queda de tensão," *Controle and Automacao*, pp. 150–159, 2000.

[20] C. Coffrin, R. Bent, K. Sundar, Y. Ng, and M. Lubin, "Powermodels.jl: An open-source framework for exploring power flow formulations," in *2018 Power Systems Computation Conference (PSCC)*, June 2018, pp. 1–8.